Journal of Magnetic Resonance **154,** 280–286 (2002)
doi:10.1006/jmre.2001.2475, available online at http://www.idealibrary.com on IDEAL®

Signal Enhancement in 5QMAS Spectra of Spin-5/2 Quadrupolar Nuclei

Amir Goldbourt and Shimon Vega

Weizmann Institute of Science, Rehovot 76100, Israel

E-mail: shimon.vega@weizmann.ac.il; amir.goldbourt@weizmann.ac.il

Received July 27, 2001; revised November 2, 2001; published online January 16, 2002

5QMAS experiments on spin-5/2 systems display a low sensitivity compared with their 3QMAS counterparts. Nevertheless, the superior resolution of 5QMAS over 3QMAS makes these experiments a favorable choice for many materials. We report an enhancement scheme for the 5QMAS experiment, using an improved five-quantum excitation pulse scheme combined with a FAM-II conversion pulse. The results are verified experimentally on a polycrystalline sample of γ-$^{27}Al_2O_3$, showing an enhancement factor of 2.4 over the simple two-pulse (CW) 5QMAS scheme. Numerical computations of the efficiency parameter ϵ support these results. © 2002 Elsevier Science (USA)

Key Words: **solid state NMR; MQMAS; FAM; quadrupolar nuclei; sensitivity enhancement.**

1. INTRODUCTION

High-resolution solid state NMR of noninteger spins with $I > 1/2$ can be achieved using the multiple-quantum magic-angle-spinning (MQMAS) experiment, introduced by Frydman and Harwood (*1*). This method is based on exciting multiple-quantum coherences and subsequently converting them into observable single-quantum coherences. Although these processes can be successfully performed on single crystals (*2–4*), their applicability to powder samples is limited, due to their wide range of quadrupolar frequencies. Hence, the sensitivity of MQMAS is low. Various ways for enhancing MQMAS signals have been suggested in the literature. The original two-pulse excitation scheme (*1*) was initially replaced by a one-pulse excitation (*5–7*). The efficiency of the multiple-quantum excitation generated by this pulse was studied thoroughly as a function of various NMR parameters such as radio-frequency (RF) power, sample spinning rate, and RF offset. Consequently, values were suggested for the practical implementation of MQMAS experiments (*8, 9*). Synchronization of the pulses with the rotor period proved efficient (*10*) but limits the spectral width in the MQMAS experiment. During QCPMG (*11*) experiments that are based on the Carr–Purcell–Meiboom–Gill echo sequence, the central transition MAS echoes following the MQMAS sequence are successively accumulated to enhance the overall signal intensity. This approach generates sidebands along the F_2 MAS dimension. In other schemes, signal enhancement is obtained via modification of the excitation and conversion pulses. Decaying pulses (*12, 13*), composite pulses (*14*), spin–lock pulses (RIACT-II) (*15*), double-frequency sweeps (DFS) (*16*), fast-amplitude modulation (FAM-I) (*17*) and combinations of RIACT and FAM-I (*18*), rotary resonances (FASTER-MQMAS) (*19*), combinations of rotor assisted population transfer (RAPT) (*20*) with RIACT(II) (*21*) or with SL-FAM (*22*) were all used to enhance the 3QMAS signals of spin-3/2 systems. Some of these sequences benefit from adiabatic level crossings of the central or satellite transitions in the quadrupolar spin systems (*23, 24*). In Ref. (*25*) and (*18*) several enhancement techniques are presented and compared. In (*18*) an efficiency parameter ϵ was introduced, which can assist in comparing signal amplitudes of MQMAS two-dimensional experiments. An ϵ parameter can easily be calculated for each MQMAS experiment, because it involves only the experimental parameters defining the RF excitation and conversion pulses. Based on this approach, we derived the efficient 3QMAS hybrid scheme, SL-FAM, combining a spin–lock excitation pulse from the RIACT experiment with an extended FAM-I conversion pulse.

Upon increasing the spin number 3QMAS (*1*), 5QMAS (*26*), and 5Q/3Q MQMAS (*27*) experiments were performed on samples containing spin-5/2 nuclei. Whereas the first experiment has the highest sensitivity, the latter two show a significant improvement in resolution (*27, 28*), but lack signal-to-noise. Sensitivity enhancement in 5QMAS is therefore greatly desired. For 3QMAS experiments, efforts have been mainly focused on the improvement the 3Q-to-1Q coherence ($3QC \rightarrow 1QC$) conversion process. Three pulse schemes that were introduced in that context are DFS (*16*), FAM-II (*29*), and FAM-I (*30*). Recently, it was shown that using multiple frequency sweeps (MFS) to induce population transfer, initial excitation of 3Q coherence could be improved as well (*31*). Signal enhancement in 5QMAS spectra has been achieved using fast amplitude modulation pulses (*30*) and chirped conversion pulses (*32*). However, the poor 5Q coherence excitation

1090-7807/02 $35.00

is still a limiting factor of these 5QMAS experiments. Signal enhancement in single-quantum CP-MQMAS was obtain using FAM-II pulses to induce $1QC \rightarrow 3QC$ transfer (*33*).

Here we introduce a new enhancement scheme by improving the excitation pulse and combining it with a $5QC \rightarrow 1QC$ FAM-II conversion pulse. This modified scheme results in a two- to three-fold enhancement of 5QMAS spectra obtained by a simple two-pulse excitation-conversion scheme. The effectiveness of the new sequence is confirmed by calculations and experiments.

2. EXPERIMENTAL

Phase-modulated whole-echo split-t_1 (*34*) experiments were performed on a Bruker CXP300 NMR spectrometer, controlled by a TECMAG operating system, using a 4 mm WB double-resonance Bruker MAS probe. The Larmor frequency of ^{27}Al for this spectrometer is 78.2 MHz. The pulse sequences used in this study are shown in Fig. 1. In the 5QMAS experiment the dephasing of 5Q coherences during a time $\frac{1}{1+k}\tau$ is refocused via the evolution of 1Q coherences for a time $\frac{k}{1+k}\tau$. Shifting the echo by a time τ_{echo} ensures the collection of the whole echo during acquisition and its appearance at a fixed position in the t_2 time domain. In the 2D 5QMAS experiments (for spin $\frac{5}{2}, k = \frac{25}{12}$), time increments of $\frac{12}{37}\Delta t_1$ and $\frac{25}{37}\Delta t_1$ are used for the first and second parts of the split-t_1 evolution period, respectively. The following additional parameters were used in these experiments:

Data points ($t_1 \times t_2$)	16×512
Dwell times ($\Delta t_1 \times \Delta t_2$)	$(30.83 \times 10)\,\mu$s
RF power	$\nu_1 = 91$ kHz
CW excitation pulse	$4.5\,\mu$s
CW conversion pulse	$2.1\,\mu$s
CFF excitation pulse	$\{4.5 + 4 \times (\overline{0.6}; 0.6)\}\,\mu$s
CFF conversion pulse	$\{\overline{2.1}; 1.8; \overline{1.1}; 0.8; \overline{1.4}; 0.8\}\,\mu$s
Echo pulse	$7\,\mu$s ($\nu_1 \approx 18$ kHz)
Echo delay (τ_{echo})	1 ms
Spinning frequency	10 kHz
Relaxation delay	300 ms
Reference compound	1.0 M $Al(NO_3)_3$ at 0 ppm

CW and CFF stand for the split-t_1 whole-echo versions of the CW-5QMAS sequence and the enhanced CW-FAM excitation/FAM conversion sequence, respectively, shown in Fig. 1. All segments of the FAM pulses have the same phase with positive and negative (bars) amplitudes. A Fourier transformation was performed according to reference (*34*), and the F_2 and F_1 axes were shifted by

$$\Delta \quad \text{and} \quad \frac{-p+k}{1+k}\Delta, \quad \text{respectively,}$$

where Δ is the reference frequency in ppm. For the 5QMAS experiment on a spin-5/2, $p = -5$, hence a shift of $\frac{85}{37}\Delta$ along F_1 was applied.

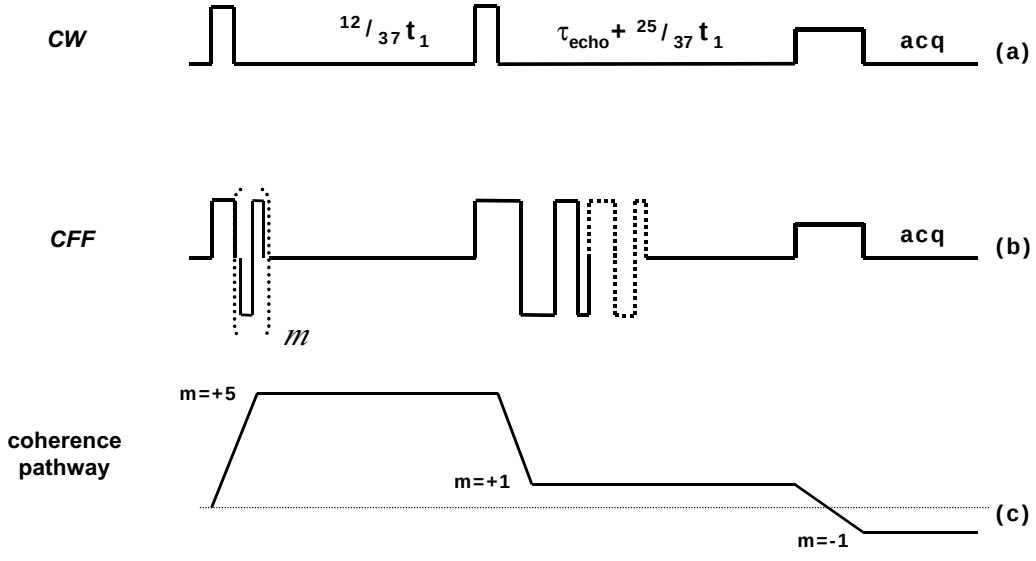

FIG. 1. Shifted-echo split-t_1 pulse schemes for 5QMAS experiments. The CW scheme (a) contains two short pulses with constant amplitudes for 5QC excitation and $5QC \rightarrow 1QC$ conversion. The CFF scheme in (b) is composed of two shaped pulses. The additional third pulse is a soft Hahn-echo π pulse. The delays between the first and second pulse and the second and third pulse are incremented simultaneously by $\frac{12}{37}\Delta t_1$ and $\frac{25}{37}\Delta t_1$, respectively. Data acquisition starts immediately after the third pulse. In (c) the coherence pathway for both sequences is shown.

The following phase cycling scheme was used to select the $(+5) \rightarrow (+1) \rightarrow (-1)$ coherence pathway (160 phases):

Phase	Values in degrees
ϕ_1	$(0, 18, 36, 54, \ldots, 342) \times 6$
ϕ_2	$(0) \times 160$
ϕ_3	$(0) \times 20, (45) \times 20, (90) \times 20, \ldots, (315) \times 20$
ϕ_r	$\{(0, 270, 180, 90) \times 5, (90, 0, 270, 180) \times 5,$ $(180, 90, 0, 270) \times 5, (270, 0, 90, 180) \times 5\} \times 2$

Pulse imperfections caused by necessary fast phase switching required experimental optimization of the FAM pulses. The FAM excitation pulse was optimized by changing the lengths and the number of the pulse segments, starting from $3 \times \{\overline{0.8}, 0.8\}$. The conversion pulse was optimized by starting with a pulse sequence $\{2, \overline{1.5}, 1, \overline{0.5}\}$, $\{1.5, \overline{1}\}$, and optimizing each step separately. Addition or substraction of segments can be employed if necessary. This procedure was exploited by monitoring the 5QMAS echo amplitude, employing a 1D scheme with a very short t_1 delay. All experiments were performed on ^{27}Al in a polycrystalline γ-Al_2O_3 sample. The RF carrier frequency was set to the octahedral site at 1.2 ppm. A large first-order phase correction of $\approx 3000^\circ$ was required in order to phase the tetrahedral site. Signal processing was done using the matNMR (*35*) program with MATLAB.

3. RESULTS AND DISCUSSION

Detailed studies of population and coherence transfer processes using modulated irradiation of the satellite lines were carried out for static single crystals (*4*) and extended to spinning single crystals and powders by Madhu *et al.* for spin-3/2 (*24*) and by Iuga *et al.* and Schäfer *et al.* for spin-5/2 (*32, 36*). It has been demonstrated that irradiation on the satellites of a rotating spin-3/2 can induce $3QC \leftrightarrow 1QC$ transfers via direct or adiabatic processes. In the same way, irradiation of the outer or inner satellite lines of a spin-5/2 can induce $5QC \leftrightarrow 3QC$ or $3QC \leftrightarrow 1QC$ transfer processes, respectively. The time dependence of the spin levels during the pulse varies for each crystallite and the level crossings affect the elements of the spin density operator in different ways. Thus, assigning one specific mechanism to these coherence transfers in rotating powder samples renders very difficult. It has been shown, however, that the populations and coherences of the MQ spin transitions can be rearranged by amplitude (FAM, RAPT) and frequency (DFS, MFS) modulated pulses. Here we exploited amplitude modulated pulses to improve the 5QMAS spectra of spins-5/2 for a large range of nuclear quadrupolar coupling constants (NQCC).

FAM Pulses in the CFF Sequence

The first pulse in the 5QMAS experiment must excite 5QC, starting from a thermal equilibrium spin state. Numerical calculations show that a short CW pulse ($<5\,\mu$s) applied to a spin-5/2 with a NQCC value of up to 12 MHz generates 3QC and, to a much lesser extent, 5QC, as depicted in Fig. 2. It is thus reasonable to assume that the addition of an irradiation on the $|\pm 3/2\rangle \leftrightarrow |\pm 5/2\rangle$ satellite transitions that induces $3QC \rightarrow 5QC$ transfer will enhance the overall 5QC. This irradiation is achieved by a fast amplitude modulation pulse with a suitable modulation frequency. Calculations of the buildup of 3QC and 5QC during the CW-FAM hybrid pulse show that different crystal orientations result in very different coherence pathways. Actually, the FAM pulse affects mainly those crystallites having a quadrupolar frequency around ω_q which matches the modulation frequency ω_m, and to a lesser extent, those in which multiples of ω_q equal ω_m. Numerical results suggest that at an RF amplitude of 90 kHz, a CW pulse of 4.5 μs combined with three $(\overline{0.6}, 0.6)$ μs pulse pairs yields a significant enhancement of the 5Q powder coherence for a range of NQCC values from 2 to 12 MHz. Similar results have been obtained using RF intensities up to $\approx$120 kHz and spinning frequencies

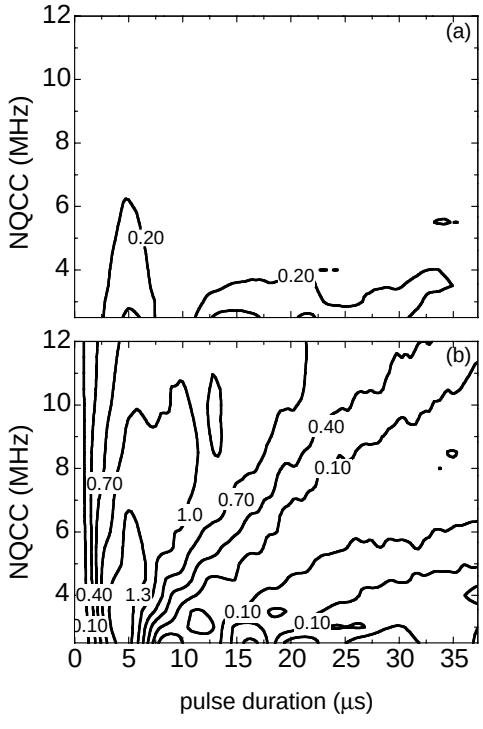

FIG. 2. Contour plots of the amplitudes of the (a) 5QC and (b) 3QC that are obtained after applying of a CW excitation pulse on a powder of spins-5/2 at thermal equilibrium. The results are shown as a function of NQCC and the pulse duration. Maximum values for the 3QC and 5QC are obtained simultaneously at $\approx$5 μs for a large range of NQCC values. In (a) most of the 5Q amplitudes are between 0 and 0.2. Powder calculations were performed employing 538 crystallite orientations using a RF field $\nu_1 = 90$ kHz and a spinning rate $\nu_r = 10$ kHz. The asymmetry parameter η was set to 0.

up to ≈25 kHz. Since both parts of the pulse are much shorter than the spinning period, the 5QC excitation of a spinning sample is very similar to the same excitation of a static sample and thus, we may refer to this pulse as a FAM-II type of irradiation.

Two types of 5QMAS conversion pulse schemes that differ from the simple CW pulse sequence have been discussed in the literature. FAM-I (*30*) and DFS (*32*) pulses were used to achieve $5QC \rightarrow 1QC$ conversion by first transferring $5QC \rightarrow 3QC$ and subsequently $3QC \rightarrow 1QC$. With FAM-I, two different modulation frequencies were successively employed and during DFS, a continuously changing frequency from the high frequency transitions $|\pm 3/2\rangle \leftrightarrow |\pm 5/2\rangle$ to the low frequency transitions $|\pm 1/2\rangle \leftrightarrow |\pm 3/2\rangle$ was utilized. Here we present yet another option based on the FAM-II type of pulses. The overall duration of these pulses is relatively short (<10 μs), with a negligible effect of the spinning on the conversion efficiency. Pulse segments are optimized numerically in two steps, first to promote $5QC \rightarrow 3QC$ and then $3QC \rightarrow 1QC$ conversion. Numerical design of the FAM-II pulse by combining the sequences $(2.5, \overline{0.6}, (0.4, \overline{0.4}) \times 4)$ μs followed by $(1.2, \overline{1.0}, 0.6, \overline{0.6})$ μs, resulted in an overall powder $5QC \rightarrow 1QC$ conversion that is enhanced over a large range of NQCC values. In Fig. 3, the powder evolution of 5QC, 3QC, and 1QC during such a FAM-II pulse, starting from a pure 5Q coherent state, is shown for two NQCC values, 5 and 8.3 MHz. The decrease of 5QC and the increase of 1QC with the intermediate 3QC can easily be recognized. The combination of this conversion FAM-II pulse with the CW-FAM-II excitation pulse, which we derived, forms the basis of our CFF experiments that yield enhanced signals in 5QMAS NMR.

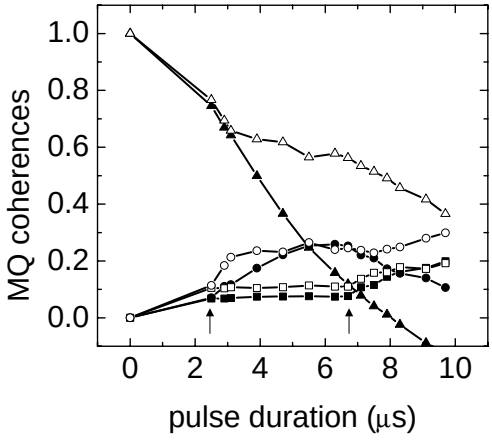

FIG. 3. The time dependence of the $5QC \rightarrow 1QC$ conversion during a FAM-II pulse. The triangles follow the evolution of the real part of the 5QC, the circles of 3QC, and the squares of 1QC. The filled and empty symbols denote spins-5/2 with NQCC values equal to 8.3 and 5 MHz, respectively. The first arrow indicates the end of a simple CW pulse and the second arrow denotes the onset of the $3QC \rightarrow 1QC$ conversion. The FAM-II pulse consists of the following segments (in μs): $2.5, \overline{0.6}, 4 \times (0.4, \overline{0.4}), 1.2, \overline{1.0}, 0.6, \overline{0.6}$.

A Comparison between 5QMAS Experiments

It has been recently shown that the intensity of MQMAS echo signals can be estimated by evaluating a single efficiency parameter ϵ for each type of experiment (*18*). The ϵ values depend solely on the excitation and conversion pulses of the MQMAS pulse sequence and can therefore be calculated straightforwardly. Calculation of ϵ for different pulse schemes therefore provides an easy way to compare their signal intensities. The parameter equals

$$\epsilon = \frac{1}{16\pi^2}\sqrt{\left[\int d\Omega \epsilon_x(\Omega)\right]^2 + \left[\int d\Omega \epsilon_y(\Omega)\right]^2}, \qquad [1]$$

where Ω represents the initial orientation of the quadrupolar principal axis system of the crystallites in the rotor frame. Taking into account only the echo coherence pathway, and assuming rotor synchronized t_1 values in the 2D MQMAS experiments, the $\epsilon_{x,y}(\Omega)$ coefficients are

$$\begin{aligned} \epsilon_x(\Omega) &= e_x(c_{xx} + c_{yy}) + e_y(c_{yx} - c_{xy}) \\ \epsilon_y(\Omega) &= e_y(c_{xy} - c_{yx}) + e_x(c_{xx} + c_{yy}). \end{aligned} \qquad [2]$$

The coefficients in these expressions denote the amount of multiple-quantum coherences obtained after the excitation pulse ($e_{x,y}$), starting from a spin system in thermal equilibrium, and the single-quantum coherences following a $MQC \rightarrow 1QC$ transfer, starting from MQC in the x direction (c_{xx}, c_{xy}), and in the y direction (c_{yx}, c_{yy}). Hence, we performed ϵ calculations for the CW and CFF sequences appearing in Fig. 1. In the calculations, first and second order quadrupolar terms are included in the Hamiltonian, and the results are shown in Fig. 4. In addition to the CW and CFF experiments, the results for different combinations of excitation and conversion pulses are shown. The FAM-I scheme introduced by Vosegaard *et al.* (*30*) indeed results in a significant enhancement. Using FAM-II only for excitation (circles) or conversion (diamonds) results in a larger ϵ value compared to the simple CW scheme. However, the CFF sequence shows the largest ϵ over the whole range of NQCC considered.

Experimental Results

Skyline projections of the ^{27}Al-5QMAS 2D spectra on the isotropic frequency axis obtained by the CW and CFF experiments are shown in Fig. 5a. A signal enhancement of the CFF scheme can be observed with a factor of 2.4 between the two results for the octahedral site (≈50 ppm). The tetrahedral site (≈180 ppm), which could hardly be distinguished from the noise in the CW spectrum, is clearly observed in the CFF spectrum. From the position of the maximum signal in the two-dimensional MQMAS spectrum, it is possible to extract the chemical shift (δ_{cs}) as well as the second order quadrupole effect parameter (SOQE $\equiv e^2qQ/\hbar\sqrt{1+\eta^2/3}$). Their general expressions, derived from δ_1 and δ_2, depend on the coherence order

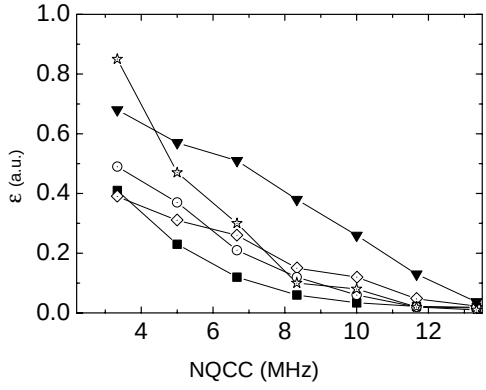

FIG. 4. The ϵ values of various 5QMAS schemes are shown. The filled triangles and squares represent the results of the CFF and CW sequences of Fig. 1, respectively. The stars denote the results of the CW-FAM-I sequence, suggested by Vosegaard *et al.* (*30*). Also drawn are results from a CW excitation/FAM-II conversion (diamonds) and a CW-FAM-II excitation/CW conversion (circles) experiments. The following pulse lengths were used: CW excitation pulse 4.5 μs, FAM-II excitation sequence $5 \times (\overline{0.6}, 0.6)$, FAM-II conversion sequence (as in Fig. 3) 2.5, $\overline{0.6}$, $4 \times (0.4, \overline{0.4})$, 1.2, $\overline{1.0}$, 0.6, $\overline{0.6}$ and FAM-I conversion sequence $6 \times (0.4, \textit{0.4}, \overline{0.4}, \textit{0.4})$, $4 \times (0.85, \textit{0.85}, \overline{0.85}, \textit{0.85})$. The numbers in italics represent delays and all others pulse lengths. Other calculation details are as in Fig. 2.

m and the spin quantum number I, and are

$$\delta_{cs} = -\frac{(1+k)A^I_{-1}}{pA^I_{-1}+A^I_p}\delta_1 + \frac{A^I_p + kA^I_{-1}}{pA^I_{-1}+A^I_p}\delta_2 \quad [3]$$

$$\delta_q = \frac{1+k}{pA^I_{-1}+A^I_p}\delta_1 + \frac{p-k}{pA^I_{-1}+A^I_p}\delta_2, \quad [4]$$

where $p = -m$ for a coherence order $m = 2I$ and $p = m$ for $m < 2I$. In these equations

$$A^I_n = \frac{n}{30}(4I(I+1) - 3n^2) \quad [5]$$

$$k = p \cdot \frac{36I(I+1) - 17p^2 - 10}{36I(I+1) - 27}. \quad [6]$$

The value of SOQE can then be derived from δ_q (in ppm) and ω_L, the Larmor frequency,

$$SOQE = \frac{\omega_L/2\pi}{10^3}\sqrt{\delta_q} \times \frac{4I(2I-1)}{3}. \quad [7]$$

For a 5QMAS experiment on a spin $I = 5/2$, we get that $p = -5$ and $k = 25/12$, and Eqs. [3] and [4] reduce to

$$\delta_{cs} = \frac{37}{135}\delta_1 + \frac{10}{27}\delta_2 \quad [8]$$

$$\delta_q = \frac{37}{144}\delta_1 - \frac{85}{144}\delta_2. \quad [9]$$

From the peak position in the CFF-5QMAS 2D contour plot in Fig. 5b, δ_1 and δ_2 for the γ-Al_2O_3 sample are 41.4 and 1.2 ppm, respectively. Insertion into Eqs. [8] and [9] yields a chemical shift of 12 ppm and a SOQE parameter of 3.3 MHz. This value corresponds to an NQCC value between 3.3 ($\eta = 0$) and 3.8 ($\eta = 1$) MHz.

Initial Population Transfer

The application of amplitude and frequency modulated pulses is not restricted to coherence transfer alone and was successfuly

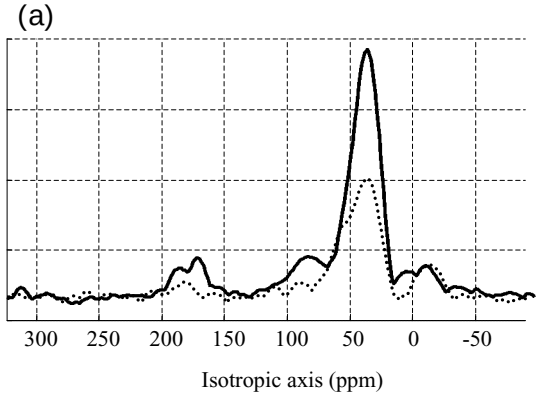

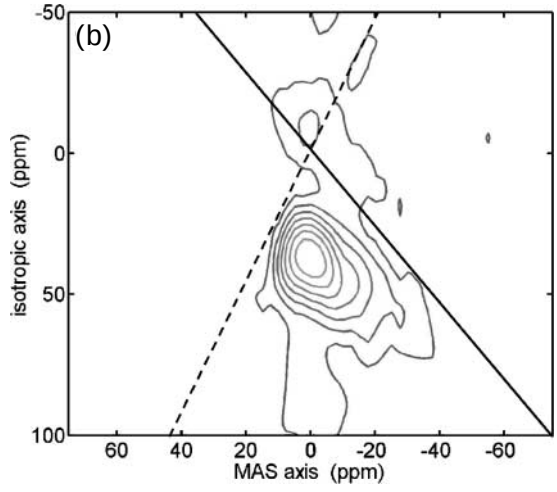

FIG. 5. (a) Skyline projections along the isotropic axis obtained from the CFF (solid line) and CW (dotted line) 2D spectra. Octahedral and tetrahedral sites are located arount 50 and 180 ppm, respectively. (b) The octahedral region of the CFF-5QMAS 2D Fourier transform spectrum obtained from a split-t_1 whole-echo experiment on ^{27}Al in a polycrystaline sample of γ-Al_2O_3. Seven contours are drawn between 10 and 85% of the maximum value. Lines with $\delta_{cs} = 0$ (solid) and $\delta_q = 0$ (dash) are drawn for reference. The values of the chemical shift (12 ppm) and SOQE (3.3 MHz) were derived from the peak position in the 2D contour plot.

used for population transfer as well (*20*). Signal enhancement of 60–100% in the MQMAS of spin-3/2 was obtained by rearranging the populations prior to the RIACT sequence (*21*) and the SL-FAM sequence (*22*). Recently it was demonstrated that it is possible to enhance the triple-quantum excitation by applying a population transfer pulse on the outer satellites of a spin-5/2 (*31*), using 2–4 multiple frequency sweeps. The enhancement that could be achieved was of the order of only 20–25% (out of a theoretical 67%) in the 3QMAS experiment. We examined the feasibility of achieving population transfer in a spin-5/2 using FAM irradiation ($x\,\bar{x}$). Since in the CFF-5QMAS experiment we rely on the initial 3Q rather then the 5Q excitation, a similar signal gain was expected, if the FAM pulses are as efficient as the MFS pulses. We therefore performed numerical calculations comparing the amount of 5QC excitation with and without the preparation pulse. We employed a FAM modulation of $\omega_m = 1$ MHz and a RF field of 50 kHz, which resulted in a signal enhancement of 10–20% for NQCC values between 6 and 10 MHz. For values below 6 MHz, the enhancement gradually decreases toward 0%, whereas above 11 MHz a signal reduction was observed. However, in the MAS spectra, an enhancement of 50–100% was observed for NQCC > 7 MHz at high RF amplitudes ($\nu_1 \approx 100$ kHz).

4. CONCLUSIONS

We have demonstrated a method to enhance the signal of 5QMAS experiments on spin-5/2 systems, using FAM-II pulses for the 5QC excitation and $5QC \rightarrow 1QC$ conversion. Improved excitation was obtained by using the relatively large 3QC, created by a simple CW pulse, and converting it to 5QC via a FAM-II irradiation on the $|\pm 3/2\rangle \leftrightarrow |\pm 5/2\rangle$ satellite transitions. The conversion pulse consists of two parts that sequentially promote $5QC \rightarrow 3QC$ and $3QC \rightarrow 1QC$ processes. This last pulse can also be replaced by suitable FAM-I or DFS pulses as well.

ACKNOWLEDGMENTS

The authors thank P. K. Madhu for fruitful discussions. This research was supported by the Israel–US Binational Science Foundation.

REFERENCES

1. L. Frydman and J. S. Harwood, Isotropic spectra of half-integer quadrupolar spins from bidimensional magic-angle spinning NMR, *J. Am. Chem. Soc.* **11,** 5367–5368 (1995).
2. S. Vega, Fictitious spin 1/2 operator formalism for multiple quantum NMR, *J. Chem. Phys.* **68**(12), 5518–5527 (1978).
3. A. Wokaun and R. R. Ernst, Selective excitation and detection in multilevel spin systems: Application of single transition operators, *J. Chem. Phys.* **4,** 1752–1758 (1977).
4. S. Vega and Y. Naor, Triple quantum NMR on spin systems with I = 3/2 in solids, *J. Chem. Phys.* **75**(1), 75–86 (1981).
5. C. Fernandez and J. P. Amoureux, Triple-quantum MAS-NMR of quadrupolar nuclei, *Solid State Nucl. Magn. Reson.* **5,** 315–321 (1996).
6. A. Medek, J. S. Harwood, and L. Frydman, Multiple-quantum magic-angle spinning NMR: A new method for the study of quadrupolar nuclei in solids, *J. Am. Chem. Soc.* **117,** 12,779–12,787 (1995).
7. G. Wu, D. Rovnyak, S. Boqin, and R. G. Griffin, High resolution multiple quantum MAS NMR spectroscopy of half-integer quadrupolar nuclei, *Chem. Phys. Lett.* **249,** 210–217 (1995).
8. J. P. Amoureux, M. Pruski, D. P. Lang, and C. Fernandez, The effect of RF power and spinning speed on MQMAS NMR, *J. Magn. Reson.* **131**(1), 170–175 (1998).
9. J. P. Amoureux, C. Fernandez, and L. Frydman, Optimized multiple-quantum magic-angle spinning NMR experiments on half-integer quadrupoles, *Chem. Phys. Lett.* **259**(3-4), 347–355 (1996).
10. D. Massiot, Sensitivity and lineshape improvement of MQ-MAS by rotor-synchronized data acquisition, *J. Magn. Reson. Ser. A* **122,** 240–244 (1996).
11. F. H. Larsen, H. J. Jakobsen, P. D. Ellis, and N. C Nielsen, QCPMG-MAS NMR of half-integer quadrupolar nuclei, *J. Magn. Reson.* **131,** 144–147 (1998).
12. S. H. Ding and C. A. McDowell, Shaped pulse excitation in multi-quantum magic-angle spinning spectroscopy of half-integer quadrupole spin systems, *Chem. Phys. Lett.* **270,** 81–86 (1997).
13. S. Ding and C. A. McDowell, Multiple-quantum MAS NMR spectroscopy of spin-3/2 quadrupolar spin systems using shaped pulses, *J. Magn. Reson.* **135,** 61–69 (1998).
14. L. Marinelli and L. Frydman, Composite pulse excitation schemes for MQMAS NMR of half-integer quadrupolar nuclei, *J. Magn. Reson.* **132,** 88–95 (1998).
15. G. Wu, D. Rovnyak, and R. G. Griffin, Quantitative multiple-quantum magic-angle-spinning NMR spectroscopy of quadrupolar nuclei in solids, *J. Am. Chem. Soc.* **118,** 9326–9332 (1996).
16. A. P. M. Kentgens and R. Verhagen, Advantages of double frequency sweeps in static, MAS and MQMAS NMR of spin I = 3/2 nuclei, *Chem. Phys. Lett.* **300,** 435–443 (1999).
17. P. K. Madhu, A. Goldbourt, L. Frydman, and S. Vega, Sensitivity enhancement of the MQMAS NMR experiment by fast amplitude modulation of the pulses, *Chem. Phys. Lett.* **307,** 41–47 (1999).
18. A. Goldbourt, P. K. Madhu, S. Kababya, and S. Vega, The influence of the radio-frequency excitation and conversion pulses on the intensities and lineshapes of the triple-quantum MAS NMR spectra of I = 3/2 nuclei. *Solid State Nucl. Magn. Reson.* **18,** 1–16 (2000).
19. T. Vosegaard, P. Florian, D. Massiot, and P. J. Grandinetti, Multiple-quantum magic-angle spinning using rotary resonance excitation, *J. Chem. Phys.* **114**(10), 4618–4624 (2001).
20. Z. Yao, H.-T. Kwak, D. Sakellariou, L. Emsley, and P. J. Grandinetti, Sensitivity enhancement of the central transition NMR siganl of quadrupolar nuclei under magic-angle spinning, *Chem. Phys. Lett.* **327,** 85–90 (2000).
21. H. T. Kwak, S. Prasad, Z. Yao, P. J. Grandinetti, J. R. Sachleben, and L. Emsley, Enhanced sensitivity in RIACT/MQ-MAS NMR experiments using rotor assisted population transfer, *J. Magn. Reson.* **150,** 71–80 (2001).
22. P. K. Madhu and M. H. Levitt, 2nd Alpine conference on solid state NMR Chamonix–Mont Blanc, France, 2001.
23. A. J. Vega, MAS NMR spin locking of half-integer quadrupolar nuclei, *J. Magn. Reson. Ser. A* **96,** 50–68 (1992).
24. P. K. Madhu, A. Goldbourt, L. Frydman, and S. Vega, Fast radio-frequecy amplitude modulation in multiple-quantum magic-angle-spinning nuclear magnetic resonance: Theory and experiments, *J. Chem. Phys.* **112**(5), 2377–2391 (2000).
25. M. Pruski, J. W. Wiench, and J. P. Amoureux, On the conversion of triple to single quantum coherences in MQMAS NMR, *J. Magn. Reson.* **147,** 286–295 (2000).

26. C. Fernandez and J. P. Amourex, 2D multiquantum MAS NMR spectroscopy of ^{27}Al in aluminophosphate molecular sieves, *Chem. Phys. Lett.* **242,** 449–454 (1995).

27. A. Jerschow, J. W. Logan, and A. Pines, High-resolution NMR of quadrupolar nuclei using mixed multiple-quantum cohrences, *J. Magn. Reson.* **149,** 268–270 (2001).

28. K. J. Pike, R. P. Malde, S. E. Ashbrook, J. McManus, and S. Wimperis, Multiple-quantum MAS NMR of quadrupolar nuclei. Do five- seven- and nine-quantum experiments yield higher resolution that the three-quantum experiment? *Solid State Nucl. Magn. Reson.* **16,** 203–215 (2000).

29. A. Goldbourt, P. K. Madhu, and S. Vega, Enhanced conversion of triple to single-quantum coherence in the triple-quantum MAS NMR spectroscopy of spin 5/2 nuclei, *Chem. Phys. Lett.* **320,** 448–456 (2000).

30. T. Vosegaard, D. Massiot, and P. J. Grandinetti, Sensitivity enhancement in MQ-MAS NMR of spin-5/2 nuclei using modulated *rf* mixing pulses, *Chem. Phys. Lett.* **326,** 454–460 (2000).

31. D. Iuga and A. P. M. Kentgens, Triple-quantum excitation enhancement in MQMAS experiments on spin $I = 5/2$ systems, *Chem. Phys. Lett.* **343,** 556–562 (2001).

32. D. Iuga, H. Schäfer, R. Verhagen, and A. P. M. Kentgens, Population and coherence transfer induced by double frequency sweeps in half-integer quadrupolar spin systems, *J. Magn. Reson.* **147,** 192–209 (2000).

33. S. E. Ashbrook and S. Wimperis, Novel two-dimensional NMR methods that combine single-quantum cross-polarizaition and multiple-quantum MAS of quadrupolar nuclei, *Chem. Phys. Lett.* **340,** 500–508 (2001).

34. S. P. Brown and S. Wimperis, Two-dimensional multiple-quantum MAS NMR of quadrupolar nuclei acquisition of the whole echo, *J. Magn. Reson.* **124,** 279–285 (1997).

35. J. Van Beek, "matNMR Toolbox," Version 2.1; also http://www.nmr.ethz.ch/matnmr.

36. H. Schäfer, D. Iuga, R. Verhagen, and A. P. M. Kentgens, Population and coherence transfer in half-integer quadrupolar spin systems induced by simultaneous rapid passages of the sattelite transition: A static and spinning single crystal nuclear magnetic resonance study, *J. Chem. Phys.* **114**(7), 3073–3091 (2001).